Received: 2 March 2022 | Revised: 19 April 2022 | Accepted: 21 April 2022

DOI: 10.1002/ardp.202200105

FULL PAPER

ARCH PHARM DPhG
Archiv der Pharmazie

Synthesis, density functional theory calculation, molecular docking studies, and evaluation of novel 5-nitrothiophene derivatives for anticancer activity

Demokrat Nuha[1,2,3] | Asaf E. Evren[1,4] | Zennure Ş. Çiyanci[5] | Halide E. Temel[5] | Gülşen Akalin Çiftçi[5] | Leyla Yurttaş[1]

[1]Department of Pharmaceutical Chemistry, Faculty of Pharmacy, Anadolu University, Eskişehir, Turkey

[2]Department of Chemistry, Faculty of Science, Eskisehir Technical University, Eskişehir, Turkey

[3]Faculty of Pharmacy, University of Business and Technology, Prishtina, Kosovo

[4]Department of Pharmacy Services, Vocational School of Health Services, Bilecik Seyh Edebali University, Bilecik, Turkey

[5]Department of Biochemistry, Faculty of Pharmacy, Anadolu University, Eskişehir, Turkey

Correspondence
Demokrat Nuha, Department of Chemistry, Faculty of Science, Eskisehir Technical University, Eskişehir 26555, Turkey.
Email: demokratnuha@gmail.com and demokrat_nuha@eskisehir.edu.tr

Funding information
Anadolu Üniversitesi, Grant/Award Number: Project no. 2005S027

Abstract

Within the scope of this study, new 2-{2-[(5-nitrothiophen-2-yl)methylene] hydrazinyl}thiazole derivatives (**2a–j**) were synthesized and investigated for their potential anticancer and enzyme inhibition activities. Spectroscopic techniques were used to determine the structures of substances. The anticancer activities of compounds were detected in A549 human lung carcinoma and L929 murine fibroblast cell lines, determining cytotoxicity, apoptosis, mitochondrial membrane integrity, and caspase-3 activation. Compounds **2b** bearing 4-nitrophenyl, **2c** bearing phenyl, and **2d** bearing 4-cyanophenyl moieties were specified with high anticancer activity, acting through an apoptotic pathway with an apoptosis ratio of 9.61%–15.59%. Mitochondrial membrane depolarization was determined to be 25.53% and 22.33% for compounds **2b** and **2c**, respectively. Furthermore, compound **2c** exhibited excellent caspase-3 activation. A molecular docking study was realized with compound **2c** on the caspase-3 enzyme. Furthermore, the electronic characteristics of the active compounds were investigated using density functional theory (DFT) at the B3LYP/6-31G (d, p) level. The frontier molecular orbital energy and atomic net charges were examined.

KEYWORDS
anticancer activity, DFT calculation, molecular docking, thiazole, thiophene

1 | INTRODUCTION

One of the most pressing health issues today is cancer, which is defined as the uncontrolled multiplication and spread of aberrant cells.[1,2] Cancer is one of the leading causes of mortality, with approximately 9 million deaths worldwide each year.[3] Cancer morbidity and mortality have been increasing for a long time and will continue to do so.[4,5] Lung cancer accounts for 12.3% of all new cases, and therapy is highly connected to the kind and stage of the diagnosed tumor.[6,7] Chemotherapy is the mainstay of cancer treatment. However, the rapid emergence of medication resistance, as well as the severe adverse effects of commonly utilized anticancer medicines, remain major barriers to effective chemotherapy.[8,9] The ongoing exploration of anticancer medicines with minimal toxicity and great efficacy remains an important direction in anticancer drug research.[10,11]

The thiazole ring exhibits a diverse set of biological activities, including antibacterial,[12–14] analgesic,[15,16] anti-inflammatory,[17,18] antioxidant,[19,20] anti-HIV,[21,22] antiallergic,[23] and anticancer activities.[24–26] Thiazoles are one of the most effective classes of

compounds for targeted anticancer treatments. Many anticancer medicines contain the thiazole heterocycle, and various investigations have revealed that thiazole-based drugs generate a variety of therapeutically important pharmacological actions.[27,28] Several anticancer medications contain the thiazole moiety, including epothilones (cancer medications), dasatinib (used to treat leukemia), sodelglitazar, and tiazofurin (antineoplastic drug), as shown in Figure 1.[29,30] The thiazole nucleus is formed by the reaction of the thiosemicarbazone moiety, and preclinical investigations show that thiazole-based medicines have broad-spectrum antiproliferative actions with low toxicity. The thiosemicarbazone precursor of the thiazole heterocycle has also antitumor activity.[31,32] Thiosemicarbazones' anticancer effect appears to be due to an inhibition of DNA synthesis caused by a change in the reductive conversion of ribonucleotides to deoxyribonucleotides. This biological activity is frequently associated with their ability to block the enzyme ribonucleotide reductase, as shown with powerful anticancer medications such as triapine.[33,34]

Furthermore, because of its biological activity, the thiophene nucleus has received increased attention. It has been discovered in a number of potential anticancer medicines, including raltitrexed (Tomudex®), which induces DNA fragmentation and consequent cell death by inhibiting the thymidylate synthase enzyme.[35,36] In another study, thiophene-pyrimidine derivatives were synthesized and evaluated for antiproliferative efficacy against numerous cancer cell lines expressing high levels of EGF.[37]

The thiazole nucleus is also a component of numerous anticancer medications in clinical use, including dasatinib, dabrafenib, ixabepilone, patellamide A, and epothilone.[38] There have been a lot of thiazoles conjugated with heterocyclic molecules investigated as possible anticancer medicines for their VEGFR-2 kinase inhibitory action.[39,40] In another study, phthalimide-thiazole derivatives increased caspase 3/7 activity in A549 cells over 16 times more than the control.[41] In many of our previous studies, the anticancer effects of thiazole derivatives were determined especially on lung cancer.[42–44]

Based on the promising aspects indicated above, the method of this study comprises the bioactive substances thiazole and for the aim of synergism, and the synthesized compounds were tested as anticancer agents. In this study, we synthesized the compounds **2a–2j** and investigated their anticancer activity against A549 human lung carcinoma and L929 murine fibroblast cell lines. As a step forward in this study, the structural reactivity relationship (SAR) was investigated to predict reactive sites for chemical and biological applications using electron density and FMO energies.

2 | RESULTS AND DISCUSSION

2.1 | Chemistry

The compounds **2a–2j** were synthesized as summarized in Scheme 1. Initially, the 2-[(5-nitrothiophen-2-yl)methylene]hydrazinecarbothioamide (**1**) was catenated from 5-nitrothiophene-2-carbaldehyde and hydrazine carbothioamide. Then, the 2-bromo-1-phenylethanone derivatives and compound **1** were reacted in ethanol to obtain 2-{2-[(5-nitrothiophen-2-yl)methylene]hydrazinyl}thiazole derivatives (**2a–2j**) as the core structure. Compounds' structures that have been synthesized (**2a–2j**) were confirmed by ^{1}H-NMR, ^{13}C-NMR, and high-resolution mass

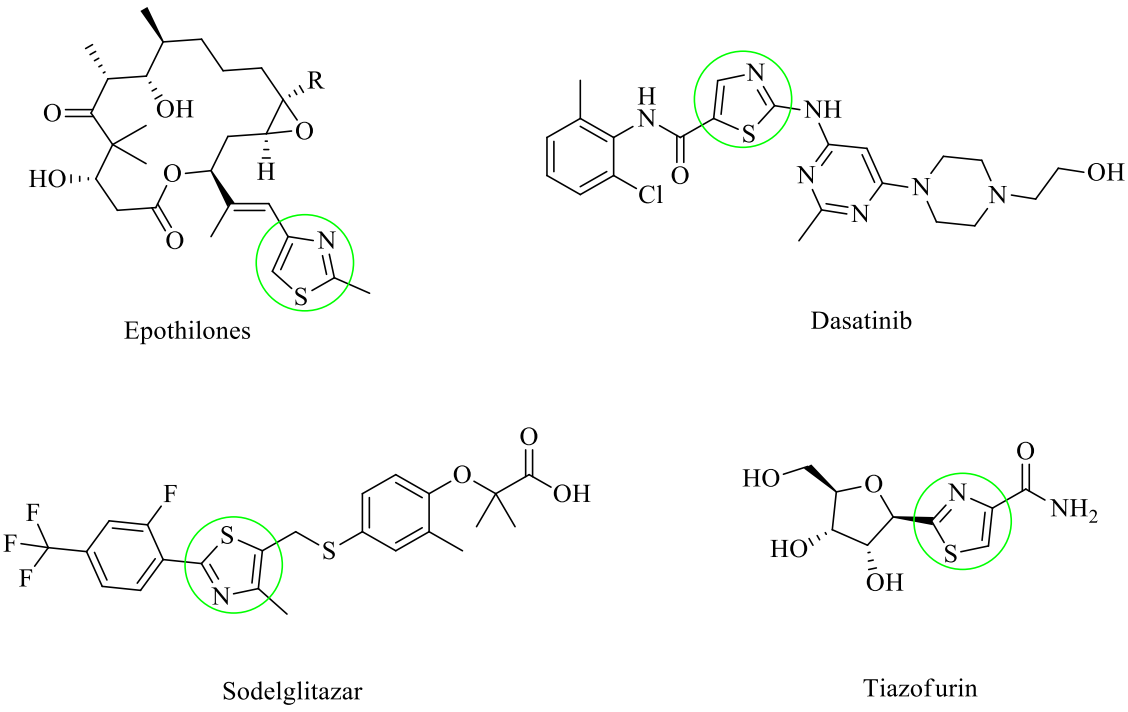

FIGURE 1 The chemical structures of drugs containing the thiazole ring.

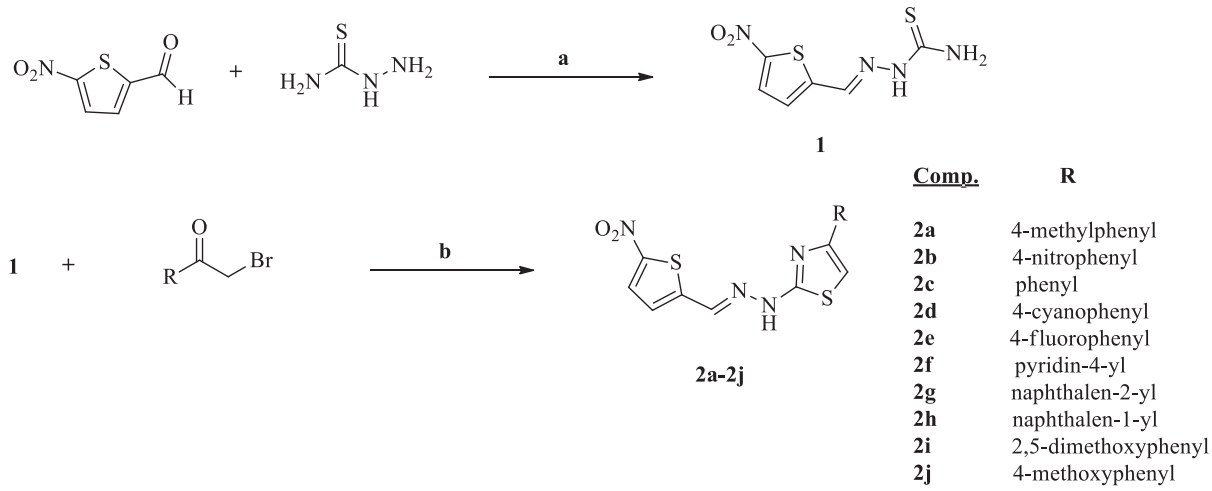

SCHEME 1 Synthesis diagram of the compounds **2a–2j**. Reagents and conditions: (a) EtOH, 80°C, 2 h; (b) EtOH, 80°C.

spectroscopy (HRMS). In the ^{1}H-NMR spectra of the aromatic and aliphatic region, the peaks were seen in estimated areas. In the ^{13}C-NMR spectra, aromatic and aliphatic regions, the peaks had been visible in the anticipated areas. The mass spectra (ESI-MS) peaks of the compounds [M +1] agreed with their expected chemical formulas (**2a–2j**).

In this investigation, we synthesized 10 novel compounds, including the 2-{2-[(5-nitrothiophen-2-yl)methylene]hydrazinyl}thiazole nucleus in their core structures. In the first step, 5-nitrothiophene-2-carbaldehyde and thiosemicarbazide were reacted for 2 h at 80°C to obtain 2-[(5-nitrothiophen-2-yl)methylene]hydrazinecarbothio-amide (**1**).[45] Then compound **1** and 2-bromo-1-phenylethanone derivatives were reacted in ethanol to gain the final products: 2-{2-[(5-nitrothiophen-2-yl) methylene]hydrazinyl}thiazole derivatives (**2a–2j**) as shown in Scheme 1. Analytical and spectral data were used to characterize all of the produced compounds. The ^{1}H-NMR spectra of compounds showed doublets at δ 7.45–8.34 ppm for thiophene protons. Thiazole proton was observed at δ 7.20–8.27 ppm as a singlet peak. Azomethine proton (H–C=N) was observed at δ 7.42–8.47 ppm as a singlet peak. The acetamide N–H proton was identified by a wide singlet signal at δ 11.83–12.99 ppm. The appearance of a pair of singlet, doublets, triplets, and/or multiplets at δ 6.84–8.10 ppm was due to the aromatic protons of the aromatic rings. The ^{13}C-NMR spectra of compounds showed signals at δ 125.94–128.93 ppm for methylene proton (H–C=N) carbon, at δ 103.18–178.59 ppm for aromatic. The computed molecular weight of the target compounds **2a–2j** was in accord with M±1 peaks in LC-MS/MS spectra.

2.2 | ADME parameters

An in silico ADME investigation of chemicals **2a–2j** was performed using the SwissADME web tool.[46,47] The five most important physicochemical factors were identified, and they are listed in Table 1. On the idea of the Lipinski "Rule of five," all the final products have good membrane permeability (BBB/GI), log *P* (2.53–4.15) ≤5, number of hydrogen bond acceptors (4–6) ≤10, molecular weight ≤500, and also the number of hydrogen bond donors (1) ≤5.[48,49] The pharmacophoric properties of the compounds indicate that they all follow and satisfy Lipinski's rule, with all attributes falling within a tolerable range. These results are consistent with the activity potency of the compounds. The synthesized molecules are expected to have a favorable pharmacokinetic profile. As a result, the compounds' drug-likeness was designated as a positive.

2.3 | Biological activity

2.3.1 | Cytotoxicity

All compounds showed higher cytotoxic activity against the A549 lung cancer cell line compared to the standard drug cisplatin (IC_{50}: 11.56 µg/ml), except compounds **2i** and **2j**. Compound **2j** also showed similar antiproliferative activity to the standard drug with a value of IC_{50}: 15.99 µg/ml. The IC_{50} value of compound **2i** containing 2,5-dimethoxyphenyl moiety could not be calculated even at the highest concentration tested (>250 µg/ml). Compounds **2a**, **2b**, **2c**, and **2d** exhibited significant cytotoxic activity against the A549 cell line (IC_{50}:6.04, 4.86, 5.25, 4.26 µg/ml, respectively) with selectivity to cancer cells. These compounds were found to be more effective than cisplatin (11.56 ± 0.38 µg/ml) (Table 2) and the cytotoxicity of the compounds on L929 cells was detected to be quite low. Other compounds **2e–2h** were not used in further anticancer activity tests since they exhibited a very high cytotoxic effect on healthy lung cell line L929 cells as well as cancer cells.

2.3.2 | Apoptosis induction

Apoptosis is a programmed cell death process that plays an important role in maintaining the regular functions and activities of cells involved in different physiological and pathological processes in the organism.[50] Compounds **2a–2d** that displayed a satisfying

TABLE 1 In silico ADME profile of our final compounds **2a**–**2j** and standard drugs

	Physicochemical properties					Pharmacokinetics		Medicinal chemistry	
	HBA	HBD	TPSA	Log $P_{o/w}$	Log *S*	GIA	Log K_p	RoF (V)	SA
2a	4	1	139.58	3.39	−7.79	Low	−4.77	Yes (0)	3.38
2b	6	1	185.40	2.53	−8.19	Low	−5.35	Yes (0)	3.31
2c	4	1	139.58	3.23	−7.40	Low	−4.95	Yes (0)	3.27
2d	5	1	163.37	2.85	−7.16	Low	−5.30	Yes (0)	3.34
2e	5	1	139.58	3.55	−7.50	Low	−4.99	Yes (0)	3.25
2f	5	1	152.47	2.54	−6.56	Low	−5.72	Yes (0)	3.23
2g	4	1	139.58	4.15	−8.70	Low	−4.37	Yes (0)	3.48
2h	4	1	139.58	4.13	−8.70	Low	−4.37	Yes (0)	3.48
2i	6	1	158.04	3.19	−7.73	Low	−5.36	Yes (0)	3.48
2j	5	1	148.81	3.23	−7.56	Low	−5.15	Yes (0)	3.28
RF-1	/	/	55.28	/	/	/	/	/	/
RF-2	4	1	41.93	1.92	−2.34	High	−6.75	Yes (0)	4.57

Abbreviations: HBA, H-bond acceptor; HBD, H-bond donor; GIA, gastrointestinal absorption; Log K_p, skin permeation (cm/s); Log $P_{o/w}$, *Consensus* Log $P_{o/w}$ (average of all five predictions); Log *S*, water solubility; RoF (V), Rule of Five (violation number); SA, synthetic accessibility from 1 (very easy) to 10 (very difficult); TPSA, topologic polar surface area (Å^2). RF-1: cisplatin, RF-2: galantamine.

TABLE 2 IC_{50} values of the compounds **2a**–**2j** against the A549 and L929 cell lines (μg/ml)

Compounds	A549	L929
2a	6.04 ± 0.46	>250
2b	4.86 ± 0.54	>250
2c	5.25 ± 0.50	62.50 ± 0.95
2d	4.26 ± 0.58	31.25 ± 0.95
2e	3.06 ± 0.32	0.90 ± 0.33
2f	3.66 ± 0.30	1.11 ± 0.73
2g	9.27 ± 0.70	1.46 ± 0.40
2h	6.45 ± 0.32	0.90 ± 0.33
2i	>250	1.90 ± 0.63
2j	15.99 ± 0.72	3.80 ± 0.49
Cisplatin	11.56 ± 0.38	-

cytotoxic profile were tested on flow cytometry to detect the apoptosis/necrosis cell ratio caused by these compounds. Compounds and cisplatin were applied at IC_{50} doses by incubating with A549 cells for 24 h. At least 10,000 cells were analyzed and evaluated on quadrants in the measurement (Figure 2). It was seen that all compounds affected A549 cells by the apoptotic pathway; compound **2b** including the 4-nitrophenyl moiety caused the highest rate of early apoptosis compared to other compounds (9.72%). The total apoptosis rate of cisplatin was 46.18%, followed by compound **2b** with a percentage of 15.59. This ratio was determined as 10.21% for compound **2d** and 9.71% for compound **2c**.

2.3.3 | Mitochondrial membrane depolarization (ΔΨm)

The compounds **2a**–**2d** were tested to detect mitochondrial membrane integrity and the results are represented in Table 3. The mitochondrial membrane depolarization was found to be 3.73%, whereas polarization was detected at 86.64%. This ratio was assigned as 37.37% and 54.37%, respectively, for cisplatin. As with the apoptotic rate, **2b** was determined as the most potent compound that caused the highest depolarization (25.53%). It was followed by **2c** with 22.33%, **2d** with 13.83%, and **2a** with 7.48%, respectively.

2.3.4 | Caspase-3 activation

Compounds **2a**–**2d**, which are the most cytotoxic compounds, were evaluated for caspase-3 activation and the findings are presented in Figure 3. The compounds **2c** with phenyl and **2d** with 4-cyanophenyl moieties were shown to cause higher caspase-3 activation compared to cisplatin. Even more, compound **2c** showed excellent activation with a percentage of 96.44%. In addition, compound **2a** with 4-methyl caused high activation of the enzyme, although not as much as cisplatin.

2.4 | Molecular docking study

Due to high-level caspase activation, we performed a molecular docking study on the caspase-3 pocket. According to the data (Figure 4), there are two hydrophobic interactions, one H-bond, and

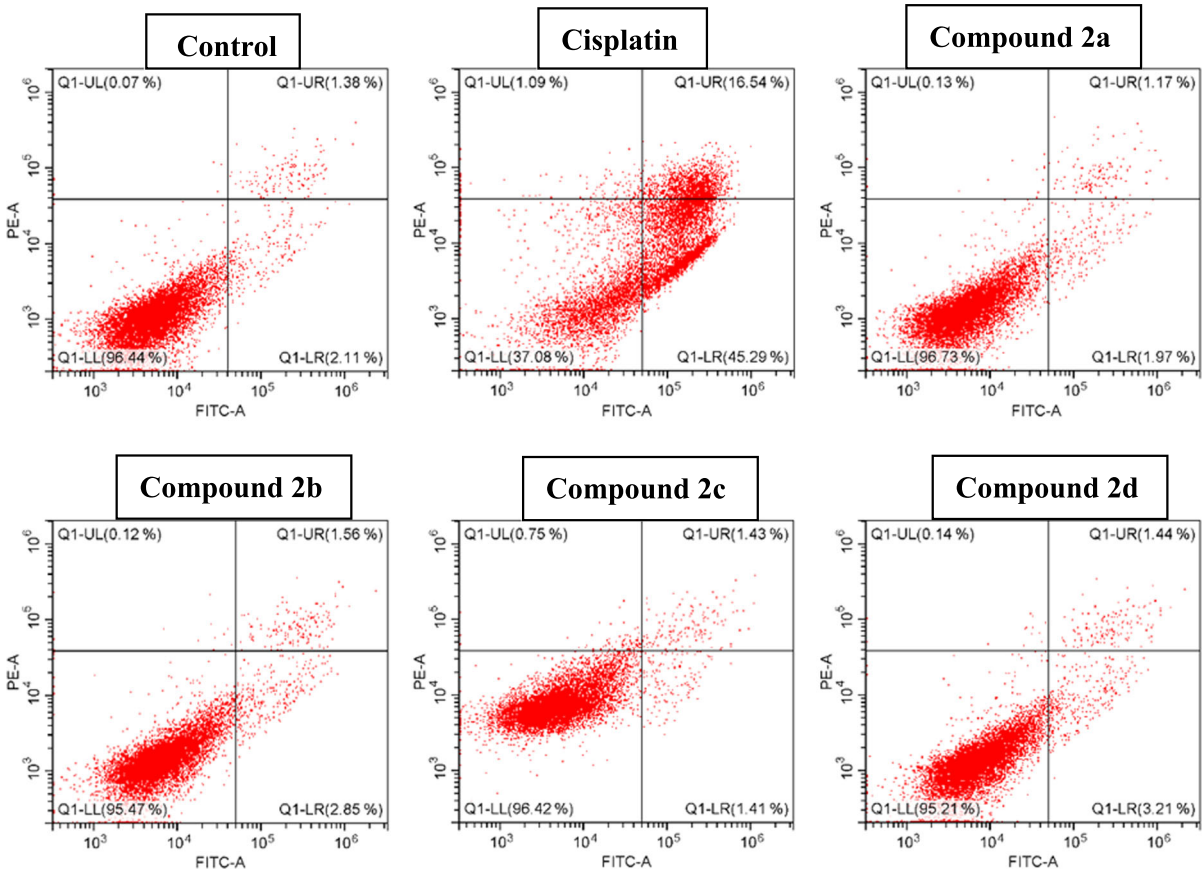

	Q1-LR (Early apoptotic)	Q1-UR (Late apoptotic)	Q1-LL (Viable)	Q1-UL (Necrotic)
Control	1.54	1.34	97.01	0.11
2a	2.31	1.79	94.19	1.71
2b	9.72	5.87	82.50	1.90
2c	6.87	2.84	72.59	17.70
2d	6.23	3.98	89.50	0.28
Cisplatin	32.36	13.82	52.98	0.84

FIGURE 2 Flow cytometry diagrams of A549 cells treated with cisplatin, compounds **2a**, **2b**, **2c**, and **2d** (necrotic, Q1; late apoptotic, Q2; viable, Q3; and early apoptotic, Q4).

TABLE 3 % Mitochondrial membrane depolarization (**2a**–**2d**)

	% Mitochondrial membrane polarized cells	% Mitochondrial membrane depolarized cells
Control	86.64	3.73
2a	87.17	7.48
2b	65.17	25.53
2c	73.82	22.33
2d	80.52	13.83
Cisplatin	54.37	37.37

two aromatic H-bonds. Compound **2c** interacted with Tyr204 and Trp206 via π–π stackings, with Arg207 via H-bond, and with Ser63 and Ser205 via aromatic H-bonds. All these amino acids were previously described as important residues to observe the activity.[51] Moreover, the docking study clarified the importance of the nitro thiophene group against the caspase-3 enzyme. Since all compounds did not have high caspase-3 activation, this common moiety could not be named as a pharmacophore group. It is obvious that there are no contacts between this group and the enzyme. However, the solvent exposure to this group is noteworthy. For this compound (**2c**), the interacted amino acids may be stabilizing the compactness of the complex, and then it may be causing the increase in bond strength. Hence, the nitro group may be choosing to face away from protein. In another scenario, the nitro group may have interacted via water-mediated H-bonds with the enzyme residues, and then it may be caused to bond more than we observed. In this case, it should have a positive effect on caspase-3 activation. In conclusion, although all these recommended scenarios were drawn forth to support the structure–activity relationship considering in vitro and in silico studies; more nitro thiophene derivatives (also its bioisosteric moiety) should be tested to finalize the structure–activity relationship.

2.5 | Results of DFT Studies

The determination of several properties of different biomolecules, such as selectivity, stability, reactivity, and some other characteristic properties, is of particular importance. In this study, we applied DFT-based global reactivity descriptors to identify these properties of the most active compounds **2b** and **2c**. The most active chemicals' three-dimensional structures are analyzed by optimizing their structures using a theoretical method without the use of any imaginary frequencies. The optimized structures of active compounds are shown in Figure 5.

The optimized geometries' frontier molecular orbital analysis was performed at the B3LYP/6-31G (d, p) level (Figure 6). The calculation of the energies of the highest occupied molecular orbital (HOMO) and lowest unoccupied molecular orbital (LUMO) determines not only the stability of the respective compounds but also enables the calculation of some of the reactivity parameters. Looking at the negative values of HOMO and LUMO, the stability of compounds **2b** and **2c** is high. Some of the reactivity parameters of the active compounds are presented in Table 4. As evidenced by the experimental findings and the values of these parameters, compound **2c** is more active. Furthermore, the most notable ionization potential (*I*) and electron affinity (*A*) values have compound **2c** with a low *I* value and compound **2b** with a high *A* value. As a result, the **2c** compound has a nucleophilic character, and the **2b** molecule has a better electrophilic character.

The tendency of an atom to attract shared electrons to itself is known as electronegativity (χ). The higher the associated electronegativity, the more electrons are attracted to an atom or a substituent group. Electro-positivity is the polar opposite of electronegativity; it is a measure of a molecule's capacity to give valence electrons. As we can see, compound **2b** has stronger electronegativity and a better electrophilic character than compound **2c**. The determination of intramolecular charge transfer of the respective compounds was calculated from the chemical hardness and softness (η, *S*) values. Compound **2c** has the highest softness and the lowest hardness value.

The determination of the potential bonds of the ligand with the biomolecules, as well as the distribution of the charges of these 3D molecules, is critical, and this is accomplished by computing the molecular electrostatic potential (MEP).[52] Figure 7 depicts the active compounds' MAP maps. The electron-rich area is highlighted in red, the electron-deficient area in blue, the moderately electron-rich area in yellow, and the neutral area in green.[53] According to the MEP mapping, the highest negative potential is found at the nitro moiety of compounds **2b** and **2c**.

Compounds were investigated for anticancer activities in A549 human lung carcinoma and L929 murine fibroblast cell lines. The SAR (structure–activity relationship) revealed that electron-withdrawing groups on aromatic rings, such as nitro, fluoro, and cyano, increase activity, whereas electron-releasing groups (–OCH_3) decrease activity against the A549 lung cancer cell line. The cytotoxic activity of the unsubstituted phenyl ring (**2c**) was also greater. These findings demonstrated that the electron-withdrawing group on the aromatic ring linked to the thiazole ring had a major impact on activity.[54,55] Compounds **2b** containing 4-nitrophenyl moieties, and **2c** containing phenyl moieties were shown to have potent antitumor action. The reason for this is hydrophobic interactions between the phenyl group and the active site in the caspase-3 binding pocket. The SAR study revealed that when various substituents (electron-releasing groups) are present in the phenyl chain, they have a deleterious impact on their activity due to their inability to properly place themselves in the caspase-3 binding region. Electron-withdrawing groups (especially the nitro group), demonstrate considerable activity due to increases in topologic polar surface area and electronegativity. This is exactly the main reason why we used nitro-thiophene in this study. This allows the chemical to engage with the improved group of caspase-3 more effectively.[44,56]

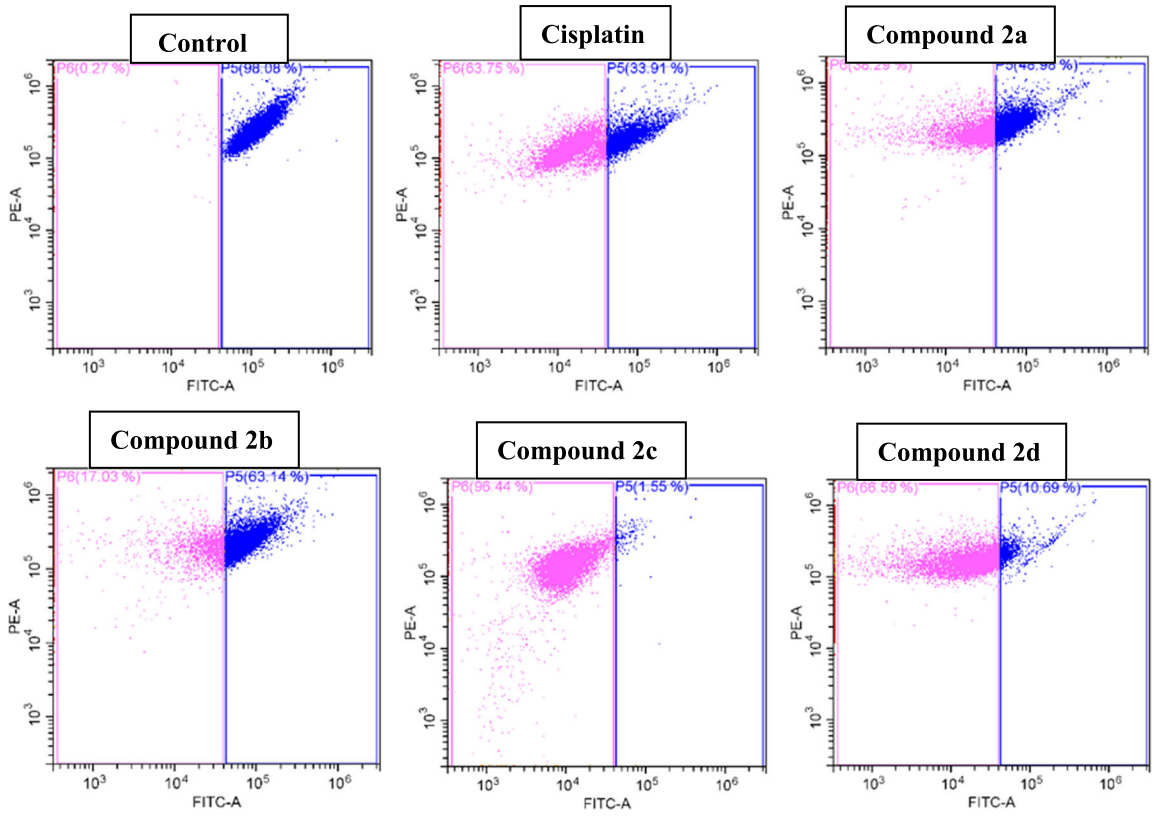

Compounds	% Caspase 3 positive cells	% Caspase 3 negative cells
Control	0.27	98.08
2a	38.29	48.98
2b	17.03	63.14
2c	96.44	1.55
2d	66.59	10.69
Cisplatin	63.75	33.91

FIGURE 3 % Caspase activation exerted by the compounds at IC_{50} doses on the A549 cell line.

3 | CONCLUSIONS

In this study, we designed and synthesized 2-{2-[(5-nitrothiophen-2-yl)methylene]hydrazinyl}thiazole derivatives (**2a**–**2j**). The anticancer and enzyme inhibitory actions of the final compounds were studied. The structures of the novel compounds were determined using spectroscopic methods such as ^{1}H-NMR, ^{13}C-NMR, and high-resolution mass spectroscopy (HRMS). Compounds **2a**–**2d** showed strong cytotoxic action against the A549 cell line with cancer cell selectivity. These compounds were found to be more effective than cisplatin, and their cytotoxicity on L929 cells was shown to be fairly minimal. Compounds **2b**–**2d** were identified as having substantial anticancer activity, operating via an apoptotic route with an apoptosis ratio of 9.61%–15.59%. As with the apoptotic rate, **2b** and **2c** were shown to be the most potent compounds, causing the most depolarization (25.53% and 22.33%, respectively). Compared to cisplatin, compounds **2c** and **2d** were observed to activate caspase-3 more. Additionally, compound **2c** showed excellent activation with a

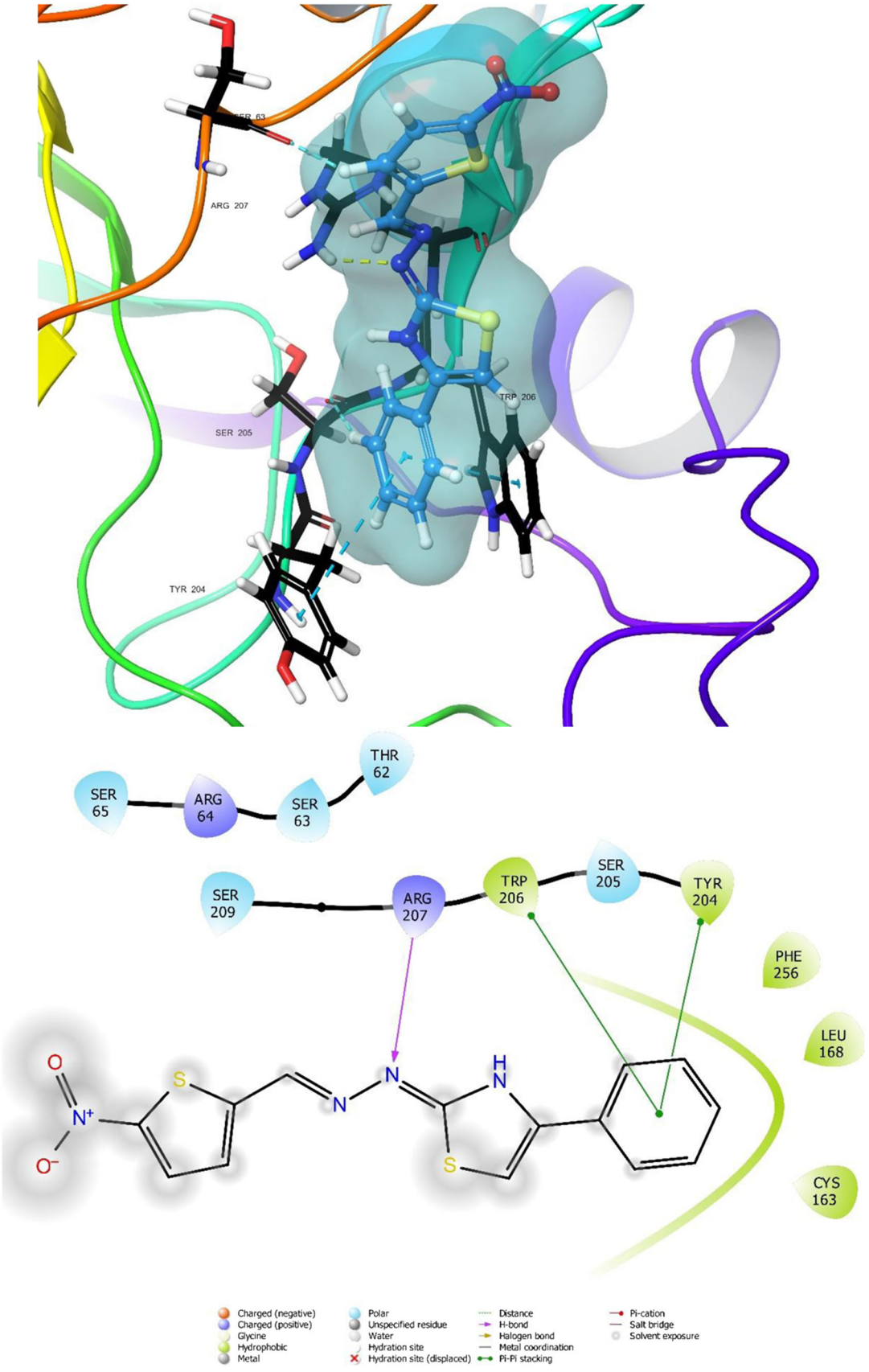

FIGURE 4 2D and 3D diagrams of the **2c**–caspase-3 enzyme complex (PDBID: 4QTX).

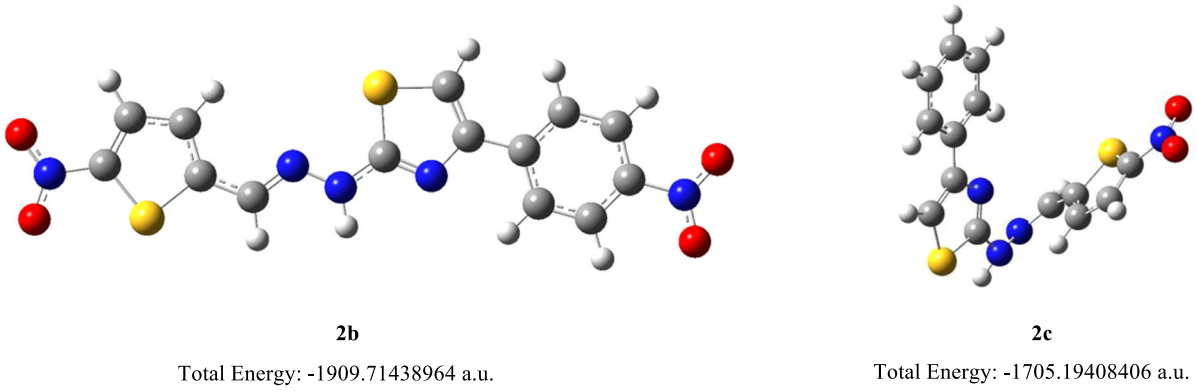

FIGURE 5 The optimized geometries of the active compounds.

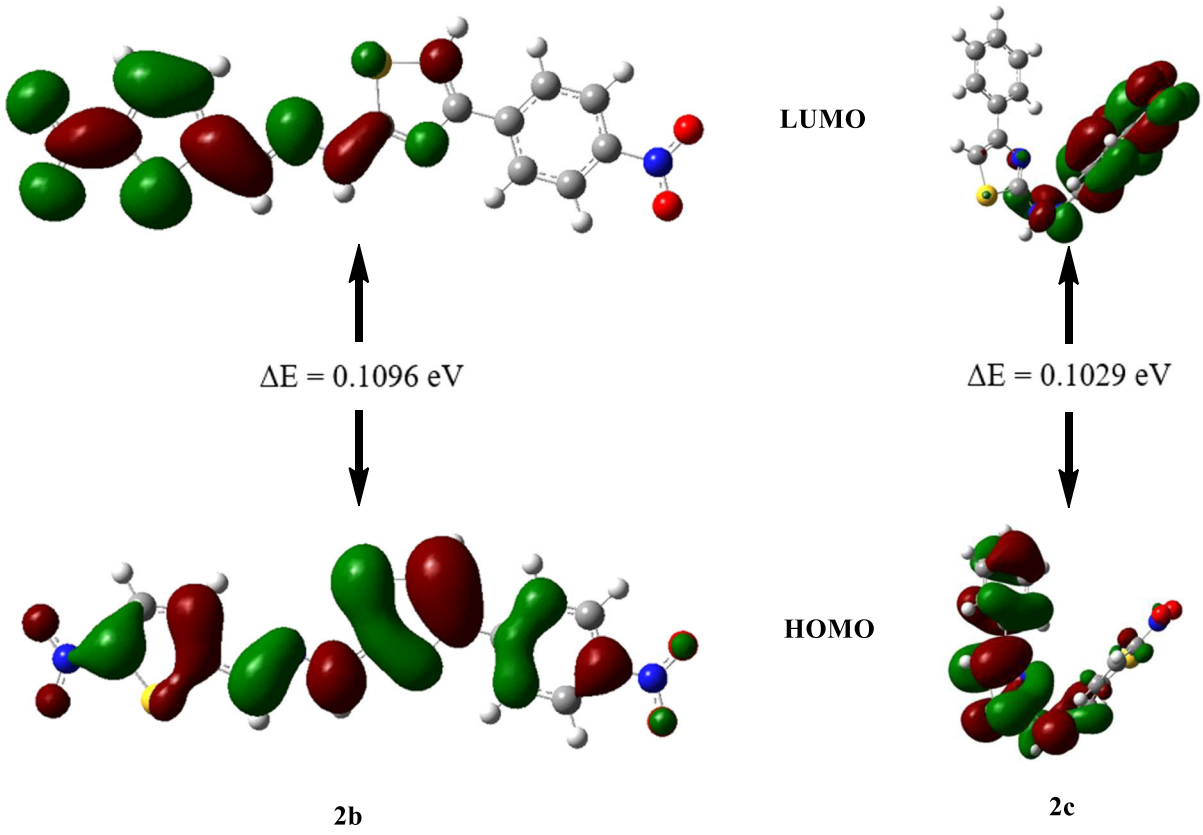

FIGURE 6 Highest occupied molecular orbital (HOMO)-lowest unoccupied molecular orbital (LUMO) diagrams of the active compounds.

TABLE 4 Some reactivity parameters of the most active compounds

Compounds	E_{HOMO} (eV)	E_{LUMO} (eV)	ΔE (eV)	I (eV)	A (eV)	χ (eV)	η (eV)	S (eV^{-1})	μ (eV)	ω (eV)
2b	−0.2242	−0.1146	0.1096	0.2242	0.1146	0.1694	0.0548	9.1241	−0.1694	0.2618
2c	−0.2121	−0.1092	0.1029	0.2121	0.1092	0.1606	0.0514	9.7276	−0.1606	0.2509

Abbreviations: HOMO, highest occupied molecular orbital; LUMO, lowest unoccupied molecular orbital.

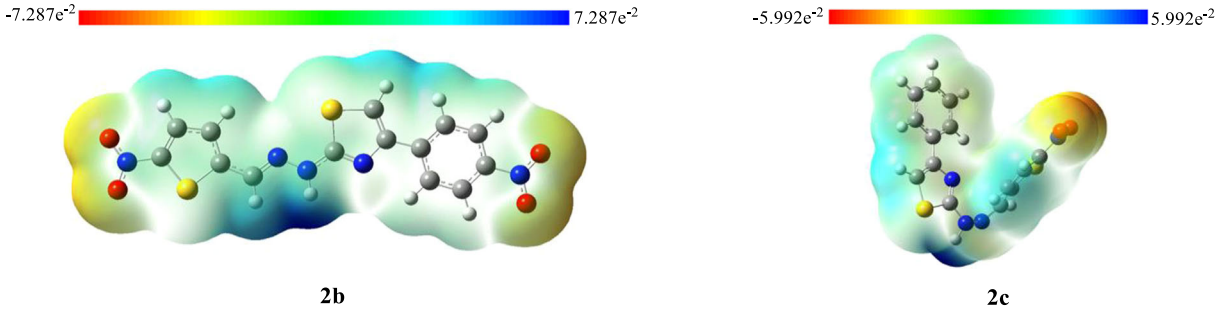

FIGURE 7 Molecular electrostatic potential surface presentation of the compounds **2b** and **2c**.

percentage of 96.44%. Molecular docking experiments on the caspase-3 enzyme were carried out for compound **2c**. Furthermore, a computational study was performed to examine the electronic properties of the active compounds using density functional theory (DFT).

4 | EXPERIMENTAL

4.1 | Chemistry

4.1.1 | General remarks

All chemical substances used in the syntheses had been bought from Merck Chemicals (Merck KGaA) or Sigma-Aldrich Chemicals (Sigma-Aldrich Corp.). The reactions and, therefore, the purities of the compounds were ascertained by thin layer chromatography (TLC) on silica gel 60 F254 aluminum sheets obtained from Merck. Melting points of the synthesized compounds had been recorded by MP90 digital melting point apparatus (Mettler Toledo) and had been provided as uncorrected. ^{1}H NMR and ^{13}C NMR spectra (see the Supporting Information) were recorded in DMSO-d_6 using a Bruker 300 and 75 MHz digital FT-NMR spectrometer (Bruker Bioscience), respectively. In the NMR spectra, the cleavage patterns were denoted as follows: s: singlet; d: doublet; t: triplet; m: multiplet. Coupling constants (*J*) are given in Hertz. High-resolution mass spectrometric (HRMS) studies were performed using an LC/MS-IT-TOF system (Shimadzu).

The InChI codes of the investigated compounds are provided as Supporting Information.

4.1.2 | Synthesis of 2-[(5-nitrothiophen-2-yl)methylene]hydrazinecarbothioamide (**1**)

Thiosemicarbazide (2.52 g, 0.03 mol) was added to a solution of 5-nitrothiophene-2-carbaldehyde (4.17 g, 0.03 mol) in ethanol (50 ml) at room temperature. The mixture was stirred for 2 h at 80°C. The reaction was monitored with TLC using silica on Al-plates and using EtOH/PE (1:3) as the mobile phase. After the reaction was completed, the precipitate was filtered off and washed with cold ethanol. m.p. 255°C–258°C[45] yield 75%.

4.1.3 | General synthesis of the 2-{2-[(5-nitrothiophen-2-yl)methylene]hydrazinyl}thiazole derivatives (**2a**–**2j**)

2-Bromo-1-phenylethanone derivatives (1.30 mmol) were added to a solution of 2-[(5-nitrothiophen-2-yl)methylene]hydrazinecarbothioamide (**1**) (0.3 g, 1.30 mmol) in ethanol (30 ml). The mixture was stirred at 80°C. The reaction was monitored with TLC using silica on Al-plates and using EtOH/PE (1:1) as the mobile phase. After the reaction was completed, the product was filtered. The final products were recrystallized from ethanol.

*2-{2-[(5-Nitrothiophen-2-yl)methylene]hydrazinyl}-4-(p-tolyl)-thiazole (**2a**)*

m. p. 221–222°C, yield 79%, ^{1}HNMR (300 MHz, DMSO-d_6, ppm) δ = 3.42 (s, 3H, –CH_3), 7.22 (d, *J* = 8.08 Hz, 1H, Ar–H), 7.40 (m, 1H, Ar–H), 7.54 (d, *J* = 4.41 Hz, 1H, Ar–H), 7.74 (d, *J* = 8.12 Hz, 1H, Ar–H), 8.06–8.10 (m, 2H, thiophene-H), 8.19 (s, 1H, thiazole-H), 8.47 (s, 1H, H–C=N), and 11.83 (brs, 1H, N–N–H). ^{13}C-NMR (75 MHz, DMSO-d_6, ppm) δ 21.27 (CH_3), 125.93, 128.19, 129.70, 130.92, 131.40, 135.71, 137.52, 147.23, 151.20, and 178.59 (S–C=N). HRMS (*m/z*): $[M+H]^+$ calculated for $C_{15}H_{12}N_4O_2S_2$: 345.0474; found 345.0460.

*4-(4-Nitrophenyl)-2-{2-[(5-nitrothiophen-2-yl)methylene]-hydrazinyl}thiazole (**2b**)*

m. p. 252–254°C, yield 82%, ^{1}HNMR (300 MHz, DMSO-d_6, ppm) δ = 7.42 (d, *J* = 4.34 Hz, 1H, Ar–H), 7.78 (s, 1H, thiazole-H), 8.05–8.09 (m, 3H, Ar–H), 8.18 (s, 1H, H–C=N), 8.25 (d, *J* = 8.83 Hz, 2H, thiophene-H), and 12.82 (brs, 1H, N–N–H). ^{13}C-NMR (75 MHz, DMSO-d_6, ppm) δ 110.22, 124.62, 126.83 (–CH=N), 128.49, 131.32, 135.24, 140.81, 146.76, 147.46, 149.21, 150.23, and 168.05 (S–C=N). HRMS (*m/z*): $[M+H]^+$ calculated for $C_{14}H_9N_5O_4S_2$: 376.0169; found 376.0172.

*2-{2-[(5-Nitrothiophen-2-yl)methylene]hydrazinyl}-4-phenylthiazole (**2c**)*

m. p. 209–210°C, yield 75%, ^{1}HNMR (300 MHz, DMSO-d_6, ppm) δ = 7.31 (d, *J* = 7.19 Hz, 1H, Ar–H), 7.37–7.40 (m, 3H, Ar–H), 7.42 (s,

1H, thiazole-H), 7.84 (d, J = 8.17 Hz, 2H, thiophene-H), 8.03 (dd, J_1 = 1.44 Hz, J_2 = 4.32 Hz, 1H, Ar–H), 8.16 (s, 1H, H–C=N), and 12.75 (brs, 1H, N–N–H). ^{13}C-NMR (75 MHz, DMSO-d_6, ppm) δ 105.29, 125.97 (–CH=N), 128.05, 128.15, 129.09, 131.23, 134.68, 147.80, 150.02, 151.01, and 167.69 (S–C=N). HRMS (m/z): $[M+1]^+$ calculated for $C_{14}H_{10}N_4O_2S_2$: 331.0318; found 331.0310.

*4-{2-{2-[(5-Nitrothiophen-2-yl)methylene]hydrazinyl}thiazol-4-yl}benzonitrile (**2d**)*

m. p. 249–251°C, yield 81%, ^{1}HNMR (300 MHz, DMSO-d_6, ppm) δ = 7.47 (d, J = 4.43 Hz,1H, Ar–H), 7.76 (s, 1H, thiazole-H), 7.88 (d, J = 8.54 Hz, 2H, Ar–H), 8.03 (d, J = 8.50 Hz, 2H, thiophene-H), 8.10 (d, J = 4.37 Hz, 1H, Ar–H), 8.22 (s, 1H, H–C=N), and 12.83 (brs, 1H, N–N–H). ^{13}C-NMR (75 MHz, DMSO-d_6, ppm) δ 109.29, 110.24, 119.42 (–CN), 126.60 (–CH=N), 128.49, 131.36, 133.24, 135.19, 138.94, 147.49, and 167.95 (S–C=N). HRMS (m/z): $[M+1]^+$ calculated for $C_{15}H_9N_5O_2S_2$: 356.0270; found 356.0272.

*4-(4-Fluorophenyl)-2-{2-[(5-nitrothiophen-2-yl)methylene]-hydrazinyl}thiazole (**2e**)*

m. p. 218–221°C, yield 76%, ^{1}HNMR (300 MHz, DMSO-d_6, ppm) δ = 7.25 (t, J = 8.91 Hz, 2H, Ar–H), 7.42–7.46 (m, 2H, Ar–H), 7.87–7.91 (m, 2H, Ar–H), 8.10 (d, J = 4.86 Hz, 1H, Ar–H), 8.20 (s, 1H, H–C=N), and 12.77 (brs, 1H, N–N–H). ^{13}C-NMR (75 MHz, DMSO-d_6, ppm) 105.21, 115.85, 116.14, 127.94 (–CH=N), 128.05, 128.27, 131.37, 134.84, 147.70, 150.08, 160.53, and 163.77 (S–C=N). HRMS (m/z): $[M+1]^+$ calculated for $C_{14}H_9FN_4O_2S_2$: 349.0224; found 349.0229.

*2-{2-[(5-Nitrothiophen-2-yl)methylene]hydrazinyl}-4-(pyridin-4-yl)thiazole (**2f**)*

m. p. 278–279°C, yield 84%, ^{1}HNMR (300 MHz, DMSO-d_6, ppm) δ = 7.50 (d, J = 4.44 Hz, 1H, pyridine-H), 8.11 (d, J = 4.35 Hz, 1H, pyridine-H), 8.27 (s, 1H, thiazole-H), 8.34 (d, J = 6.76 Hz, 2H, thiophene-H), 8.37 (s, 1H, H–C=N), 8.90 (d, J = 6.80 Hz, 2H, pyridine-H), and 12.99 (brs, 1H, N–N–H). ^{13}C-NMR (75 MHz, DMSO-d_6, ppm) δ 117.12, 122.45, 128.93 (–CH=N), 131.34, 136.09, 143.32, 146.64, 147.10, 148.74, 150.46, and 168.67 (S–C=N). HRMS (m/z): $[M+1]^+$ calculated for $C_{13}H_9N_5O_2S_2$: 332.0270; found 332.0272.

*4-(Naphthalen-2-yl)-2-{2-[(5-nitrothiophen-2-yl)methylene]-hydrazinyl}thiazole (**2g**)*

m. p. 216–217°C, yield 80%, ^{1}HNMR (300 MHz, DMSO-d_6, ppm) δ = 7.43–7.56 (m, 4H, Ar–H), 7.92–8.06 (m, 6H, Ar–H), 8.21 (s, 1H, H–C=N), and 8.37 (brs, 1H, N–N–H). ^{13}C-NMR (75 MHz, DMSO-d_6, ppm) δ 106.01, 124.29, 124.62, 126.49 (–CH=N), 126.88, 128, 128.59, 131.09, 132.12, 132.91, 133.54, 134.72, 147.75, 150.01, 150.79, and 167.74 (S–C=N). HRMS (m/z): $[M+1]^+$ calculated for $C_{18}H_{12}N_4O_2S_2$: 381.0474; found 381.0471.

*4-(Naphthalen-1-yl)-2-{2-[(5-nitrothiophen-2-yl)methylene]-hydrazinyl}thiazole (**2h**)*

m. p. 226–227°C, yield 77%, ^{1}HNMR (300 MHz, DMSO-d_6, ppm) δ = 7.20 (s, 1H, thiazole-H), 7.45 (d, J = 4.42 Hz, 1H, thiophene-H), 7.52–7.57 (m, 3H, naphthalene-H), 7.68–7.71 (m, 1H, naphthalene-H), 7.94–7.99 (m, 2H, naphthalene-H), 8.09 (d, J = 4.36 Hz, 1H, thiophene-H), 8.22 (s, 1H, H–C=N), 8.39–8.42 (m, 1H, naphthalene-H), and 12.81 (brs, 1H, N–N–H). ^{13}C-NMR (75 MHz, DMSO-d_6, ppm) δ 108.95, 125.94 (–CH=N), 126.43, 126.66, 127.43, 128.15, 128.73, 128.92, 131.02, 131.36, 133.09, 133.95, 134.83, 147.87, 150.03, and 167.51 (S–C=N). HRMS (m/z): $[M+1]^+$ calculated for $C_{18}H_{12}N_4O_2S_2$: 381.0474; found 381.0485.

*4-(2,5-Dimethoxyphenyl)-2-{2-[(5-nitrothiophen-2-yl)methylene]-hydrazinyl}thiazole (**2i**)*

m. p. 217–218°C, yield 71%, ^{1}HNMR (300 MHz, DMSO-d_6, ppm) δ = 3.73 (s, 3H, –OCH_3), 3.85 (s, 3H, –OCH_3), 6.84 (d, J = 3.21 Hz, 1H, Ar-H), 6.87 (d, J = 3.21 Hz, 1H, Ar–H), 7.02–7.05 (m, 1H, Ar–H), 7.42–7.45 (m, 1H, N–N–H), 7.50 (s, 1H, thiazole-H), 7.58 (d, J = 3.19 Hz, 1H, thiophene-H), 8.07–8.09 (m, 1H, thiophene-H), and 8.19 (s, 1H, H–C=N). ^{13}C-NMR (75 MHz, DMSO-d_6, ppm) δ 55.79 (CH3), 56.28 (CH3), 109.74, 113.20, 114.25, 116.69, 123.40, 128.13 (–CH=N), 131.35, 134.69, 147.84, 151.35, 153.37, and 166.09 (S–C=N). HRMS (m/z): $[M+1]^+$ calculated for $C_{16}H_{14}N_4O_4S_2$: 391.0529; found 391.0532.

*4-(4-Methoxyphenyl)-2-{2-[(5-nitrothiophen-2-yl)methylene]-hydrazinyl}thiazole (**2j**)*

m. p. 214–215°C, yield 89%, ^{1}HNMR (300 MHz, DMSO-d_6, ppm) δ = 3.78 (s, 3H, –OCH_3), 6.95–6.98 (m, 2H, Ar–H), 7.24 (s, 1H, thiazole-H), 7.42 (s, 1H, H–C=N), 7.77 (d, J = 3.88 Hz, 2H, Ar–H), 8.07 (d, J = 4.25 Hz, 1H, thiophene-H), 8.17 (d, J = 1.82 Hz, 1H, thiophene-H), and 12.72 (brs, 1H, N–N–H). ^{13}C-NMR (75 MHz, DMSO-d_6, ppm) δ 55.58 (CH_3), 103.18, 114.46, 127.32 (–CH=N), 127.64, 128.10, 131.35, 134.62, 147.85, 149.98, 159.36, and 167.56 (S–C=N). HRMS (m/z): $[M+1]^+$ calculated for $C_{15}H_{12}N_4O_3S_2$: 361.0424; found 361.0428.

4.2 | Biological assays

4.2.1 | MTT assay for cytotoxicity of compounds

The degree of cellular reduction of tetrazolium salt, 3-(4,5-dimethylthiazol-2-yl)-2,5-diphenyltetrazolium bromide (MTT), to formazan by mitochondrial succinate dehydrogenase was assessed in the same way as previously described in the literature with minor adjustments.[57] The MTT assay for cytotoxicity of compounds has been determined according to the previously published procedures.[43]

4.2.2 | Flow cytometric analyses of apoptosis

Compounds **2a**–**2d** with a satisfactory cytotoxic profile were examined on flow cytometry to assess apoptosis/necrosis cell ratio using previously published procedures.[58]

4.2.3 | The analysis of mitochondrial membrane potential by flow cytometry

The analysis of mitochondrial membrane potential by flow cytometry for compounds **2a–2d**, and cisplatin has been determined according to the previously published procedures.[43]

4.2.4 | Spectrofluorometric analysis of caspase-3 activation

Compounds **2a–2d**, which are the most cytotoxic compounds, were evaluated for caspase-3 activation using previously published procedures.[59]

4.3 | Prediction of physicochemical and pharmacokinetic properties

The determination of drug-like qualities, also known as the medicinal chemical profile, is critical for evaluating the proposed compounds. In this step, the pharmacokinetic profile is also predicted using in silico techniques as a preliminary evaluation. Because the current study is primarily concerned with evaluating activity, the active substances may be considered for in vivo pharmacokinetic investigations in the future.[60] As a result, the Swiss-ADME web-based application was used to determine the medicinal chemistry and pharmacokinetic profiles of the **2a–2j** compounds.[61,62]

4.4 | In silico studies

4.4.1 | Molecular docking

The crystal structure of the caspase-3 enzyme was retrieved from the Protein Data Bank server (PDBID: 4QTX). The protein preparation process, ligand preparation process, grid generation, docking, and visualization studies were performed on Schrodinger's Maestro molecular modeling package.[63–65]

The molecular docking study for compound **2c** was calculated according to the previously published procedures.[66]

4.4.2 | Density functional theory studies

The Gaussian 09W package[67] and GaussView 5.0[68–70] molecular visualization programs were used to perform theoretical approaches for our active compounds. DFT, Becke's Three-Parameter Hybrid Functional using the Lee, Yang, and Parr correlation (B3LYP)[71] method with 6–31 G(d, p) basis set in the ground state and gas phase were used to optimize the compounds' geometry. To specify intramolecular charge-transfer interactions, the HOMO and LUMO energy values of the groups of compounds were determined at a level of time-dependent (TD)-DFT.

HOMO–LUMO energy values were used to calculate chemical activity parameters such as I: ionization potential ($I = -E_{HOMO}$), A: electron affinity ($A = -E_{LUMO}$), χ: electronegativity ($\chi = (I + A)/2$), η: chemical hardness ($\eta = (I - A)/2$), S: chemical softness ($S = 1/2\eta$), μ: chemical potential ($\mu = -(I + A)/2$) and ω: electrophilicity index ($\omega = \mu^2/2\eta$) of the molecular groups.

AUTHOR CONTRIBUTIONS

Conceptualization: Leyla Yurttaş, Demokrat Nuha, and Asaf E. Evren. *Methodology*: Demokrat Nuha, Asaf E. Evren, and Zennure Ş. Çiyanci, Şevval Çiyanciennure, Şevval Çiyanci. *Software*: Demokrat Nuha and Asaf E. Evren. *Validation*: Leyla Yurttaş, Gülşen A. Çiftçi, Demokrat Nuha, Asaf E. Evren, and Halide E. Temel. *Formal analysis*: Demokrat Nuha and Asaf E. Evren. *Investigation*: Demokrat Nuha and Asaf E. Evren. *Resources*: Leyla Yurttaş, Gülşen A. Çiftçi, Demokrat Nuha, and Asaf E. Evren. *Data curation*: Leyla Yurttaş, Demokrat Nuha, and Asaf E. Evren. *Writing—original draft preparation*: Leyla Yurttaş, Demokrat Nuha, and Asaf E. Evren. *Writing—review and editing*: Gülşen A. Çiftçi, Halide E. Temel, and Zennure Ş. Çiyanci, Şevval Çiyanciennure, Şevval Çiyanci. *Visualization*: Demokrat Nuha and Asaf E. Evren. *Supervision*: Leyla Yurttaş. *Project administration*: Leyla Yurttaş. *Funding acquisition*: Leyla Yurttaş. All authors have read and agreed to the published version of the manuscript.

ACKNOWLEDGMENTS

The authors present their thanks to the DOPNA laboratory, Anadolu University and Scientific Research Projects, Anadolu University. This study was supported by the Anadolu University Scientific Research Project, Eskisehir, Turkey (Project no. 2005S027).

CONFLICTS OF INTEREST

The authors declare no conflicts of interest.

ORCID

Demokrat Nuha http://orcid.org/0000-0002-7271-6791
Asaf E. Evren https://orcid.org/0000-0002-8651-826X
Zennure Ş. Çiyanci https://orcid.org/0000-0002-2511-6689
Halide E. Temel https://orcid.org/0000-0002-5233-1165
Gülşen Akalin Çiftçi https://orcid.org/0000-0001-9535-2508
Leyla Yurttaş http://orcid.org/0000-0002-0957-6044

REFERENCES

[1] M. Govindarajan, *Eur. J. Med. Chem.* **2018**, *143*, 1208. https://doi.org/10.1016/j.ejmech.2017.10.015
[2] R. L. Siegel, K. D. Miller, A. Jemal, *CA Cancer J. Clin.* **2020**, *70*(1), 7. https://doi.org/10.3322/caac.21590
[3] M. Montana, F. Mathias, T. Terme, P. Vanelle, *Eur. J. Med. Chem.* **2019**, *163*, 136. https://doi.org/10.1016/j.ejmech.2018.11.059
[4] X. She, Y. Gao, Y. Zhao, Y. Yin, Z. Dong, *Biomed. Pharmacother.* **2021**, *140*, 111748. https://doi.org/10.1016/j.biopha.2021.111748
[5] C. G. Ethun, M. A. Bilen, A. B. Jani, S. K. Maithel, K. Ogan, V. A. Master, *CA Cancer J. Clin.* **2017**, *67*(5), 362. https://doi.org/10.3322/caac.21406

[6] J. D. Minna, J. A. Roth, A. F. Gazdar, *Cancer Cell* **2002**, *1*(1), 49. https://doi.org/10.1016/s1535-6108(02)00027-2
[7] L. G. Collins, C. Haines, R. Perkel, R. E. Enck, *Am. Fam. Physician* **2007**, *75*(1), 56.
[8] N. Chatterjee, T. G. Bivona, *Trends Cancer* **2019**, *5*(3), 170. https://doi.org/10.1016/j.trecan.2019.02.003
[9] F. Gao, X. Zhang, T. Wang, J. Xiao, *Eur. J. Med. Chem.* **2019**, *165*, 59. https://doi.org/10.1016/j.ejmech.2019.01.017
[10] U. M. Ammar, M. S. Abdel-Maksoud, C. H. Oh, *Eur. J. Med. Chem.* **2018**, *158*, 144. https://doi.org/10.1016/j.ejmech.2018.09.005
[11] C. Zhuang, X. Guan, H. Ma, H. Cong, W. Zhang, Z. Miao, *Eur. J. Med. Chem.* **2019**, *163*, 883. https://doi.org/10.1016/j.ejmech.2018.12.035
[12] S. Bondock, W. Fadaly, M. A. Metwally, *J. Med. Chem.* **2010**, *45*(9), 3692. https://doi.org/10.1016/j.ejmech.2010.05.018
[13] S. Bondock, T. Naser, Y. A. Ammar, *Eur. J. Med. Chem.* **2013**, *62*, 270. https://doi.org/10.1016/j.ejmech.2012.12.050
[14] G. M. Reddy, J. R. Garcia, V. H. Reddy, A. M. de Andrade, A. Camilo, Jr., R. A. Pontes Ribeiro, S. R. de Lazaro, *Eur. J. Med. Chem.* **2016**, *123*, 508. https://doi.org/10.1016/j.ejmech.2016.07.062
[15] R. G. Kalkhambkar, G. M. Kulkarni, H. Shivkumar, R. N. Rao, *Eur. J. Med. Chem.* **2007**, *42*(10), 1272. https://doi.org/10.1016/j.ejmech.2007.01.023
[16] G. Kumar, N. P. Singh, *Bioorg. Chem.* **2021**, *107*, 104608. https://doi.org/10.1016/j.bioorg.2020.104608
[17] S. Sinha, M. Doble, S. L. Manju, *Eur. J. Med. Chem.* **2018**, *158*, 34. https://doi.org/10.1016/j.ejmech.2018.08.098
[18] A. E. Ghonim, A. Ligresti, A. Rabbito, A. M. Mahmoud, V. Di Marzo, N. A. Osman, A. H. Abadi, *Eur. J. Med. Chem.* **2019**, *180*, 154. https://doi.org/10.1016/j.ejmech.2019.07.002
[19] B. Rosada, A. Bekier, J. Cytarska, W. Plazinski, O. Zavyalova, A. Sikora, K. Dzitko, K. Z. Laczkowski, *Eur. J. Med. Chem.* **2019**, *184*, 111765. https://doi.org/10.1016/j.ejmech.2019.111765
[20] E. D. Dincel, E. Gursoy, T. Yilmaz-Ozden, N. Ulusoy-Guzeldemirci, *Bioorg. Chem.* **2020**, *103*, 104220. https://doi.org/10.1016/j.bioorg.2020.104220
[21] H. M. Kasralikar, S. C. Jadhavar, S. V. Goswami, N. S. Kaminwar, S. R. Bhusare, *Bioorg. Chem.* **2019**, *86*, 437. https://doi.org/10.1016/j.bioorg.2019.02.006
[22] Z. Xu, M. Ba, H. Zhou, Y. Cao, C. Tang, Y. Yang, R. He, Y. Liang, X. Zhang, Z. Li, L. Zhu, Y. Guo, C. Guo, *Eur. J. Med. Chem.* **2014**, *85*, 27. https://doi.org/10.1016/j.ejmech.2014.07.072
[23] S. M. Gomha, K. D. Khalil, *Molecules* **2012**, *17*(8), 9335. https://doi.org/10.3390/molecules17089335
[24] T. I. de Santana, M. O. Barbosa, P. Gomes, A. C. N. da Cruz, T. G. da Silva, A. C. L. Leite, *Eur. J. Med. Chem.* **2018**, *144*, 874. https://doi.org/10.1016/j.ejmech.2017.12.040
[25] Y. Wang, C. Wu, Q. Zhang, Y. Shan, W. Gu, S. Wang, *Bioorg. Chem.* **2019**, *84*, 468. https://doi.org/10.1016/j.bioorg.2018.12.010
[26] T. A. Farghaly, G. S. Masaret, Z. A. Muhammad, M. F. Harras, *Bioorg. Chem.* **2020**, *98*, 103761. https://doi.org/10.1016/j.bioorg.2020.103761
[27] T. A. Farghaly, N. El-Metwaly, A. M. Al-Soliemy, H. A. Katouah, Z. A. Muhammad, R. Sabour, *Polycyclic Aromat. Compd.* **2019**, *41*(8), 1591. https://doi.org/10.1080/10406638.2019.1689512
[28] A. Ayati, S. Emami, A. Asadipour, A. Shafiee, A. Foroumadi, *Eur. J. Med. Chem.* **2015**, *97*, 699. https://doi.org/10.1016/j.ejmech.2015.04.015
[29] H. Tahtaci, M. Er, T. Karakurt, A. Onaran, *J. Heterocycl. Chem.* **2017**, *54*(1), 183. https://doi.org/10.1002/jhet.2565
[30] A. Rouf, C. Tanyeli, *Eur. J. Med. Chem.* **2015**, *97*, 911. https://doi.org/10.1016/j.ejmech.2014.10.058
[31] S. Kallus, L. Uhlik, S. van Schoonhoven, K. Pelivan, W. Berger, E. A. Enyedy, T. Hofmann, P. Heffeter, C. R. Kowol, B. K. Keppler, *J. Inorg. Biochem.* **2019**, *190*, 85. https://doi.org/10.1016/j.jinorgbio.2018.10.006
[32] Z. He, H. Qiao, F. Yang, W. Zhou, Y. Gong, X. Zhang, H. Wang, B. Zhao, L. Ma, H. M. Liu, W. Zhao, *Eur. J. Med. Chem.* **2019**, *184*, 111764. https://doi.org/10.1016/j.ejmech.2019.111764
[33] J. S. Xavier, K. Jayabalan, V. Ragavendran, A. Nityananda Shetty, *Bioorg. Chem.* **2020**, *102*, 104081. https://doi.org/10.1016/j.bioorg.2020.104081
[34] B. Z. Sibuh, S. Khanna, P. Taneja, P. Sarkar, N. K. Taneja, *Life Sci.* **2021**, *273*, 119305. https://doi.org/10.1016/j.lfs.2021.119305
[35] A. Lauria, A. Alfio, R. Bonsignore, C. Gentile, A. Martorana, G. Gennaro, G. Barone, A. Terenzi, A. M. Almerico, *Bioorg. Med. Chem. Lett.* **2014**, *24*(15), 3291. https://doi.org/10.1016/j.bmcl.2014.06.007
[36] J. F. de Oliveira, A. L. da Silva, D. B. Vendramini-Costa, C. A. da Cruz Amorim, J. F. Campos, A. G. Ribeiro, R. Olimpio de Moura, J. L. Neves, A. L. Ruiz, J. Ernesto de Carvalho, C. Alves de Lima Mdo, *Eur. J. Med. Chem.* **2015**, *104*, 148. https://doi.org/10.1016/j.ejmech.2015.09.036
[37] Z. Xiao, Z. Zhou, C. Chu, Q. Zhang, L. Zhou, Z. Yang, X. Li, L. Yu, P. Zheng, S. Xu, W. Zhu, *Eur. J. Med. Chem.* **2020**, *203*, 112511. https://doi.org/10.1016/j.ejmech.2020.112511
[38] P. C. Sharma, K. K. Bansal, A. Sharma, D. Sharma, A. Deep, *Eur. J. Med. Chem.* **2020**, *188*, 112016. https://doi.org/10.1016/j.ejmech.2019.112016
[39] L. M. Zhao, T. P. Xie, Y. Q. He, D. F. Xu, S. S. Li, *Eur. J. Med. Chem.* **2009**, *44*(4), 1410. https://doi.org/10.1016/j.ejmech.2008.09.039
[40] M. S. H. Salem, Y. M. Abdel Aziz, M. S. Elgawish, M. M. Said, K. A. M. Abouzid, *Bioorg. Chem.* **2020**, *94*, 103472. https://doi.org/10.1016/j.bioorg.2019.103472
[41] B. Donarska, M. Switalska, W. Plazinski, J. Wietrzyk, K. Z. Laczkowski, *Bioorg. Chem.* **2021**, *110*, 104819. https://doi.org/10.1016/j.bioorg.2021.104819
[42] L. Yurttaş, B. Kaya Çavuşoğlu, A. Sever, G. A. Çiftçi, *Turkish J. Biochem.* **2017**, *42*(5), https://www.degruyter.com/document/doi/10.1515/tjb-2017-0015/html
[43] L. Yurttas, H. E. Temel, M. O. Aksoy, E. F. Bulbul, G. A. Ciftci, *Drug Dev. Res.* **2021**, *83*, 470. https://doi.org/10.1002/ddr.21879
[44] A. E. Evren, L. Yurttaş, B. Ekselli, O. Aksoy, G. Akalin-Çiftçi, *Lett. Drug. Des. Discov.* **2021**, *18*(4), 372. https://doi.org/10.2174/1570180817999201022192937
[45] G. Chauviere, B. Bouteille, B. Enanga, C. de Albuquerque, S. L. Croft, M. Dumas, J. Perie, *J. Med. Chem.* **2003**, *46*(3), 427. https://doi.org/10.1021/jm021030a
[46] M. Jatczak, K. Muylaert, L. M. De Coen, J. Keemink, B. Wuyts, P. Augustijns, C. V. Stevens, *Bioorg. Med. Chem.* **2014**, *22*(15), 3947. https://doi.org/10.1016/j.bmc.2014.06.009
[47] R. Arif, M. Rana, S. Yasmeen, Amaduddin, M. S. Khan, M. Abid, M. S. Khan, Rahisuddin, *J. Mol. Struct.* **2020**, *1208*, 127905. https://doi.org/10.1016/j.molstruc.2020.127905
[48] F. A. Khan, R. H. Patil, D. B. Shinde, J. N. Sangshetti, *Bioorg. Med. Chem.* **2016**, *24*(16), 3456. https://doi.org/10.1016/j.bmc.2016.05.051
[49] Y. Isyaku, A. Uzairu, S. Uba, *Heliyon* **2020**, *6*(4), e03724. https://doi.org/10.1016/j.heliyon.2020.e03724
[50] Y. Zhang, S. Chen, C. Wei, G. O. Rankin, X. Ye, Y. C. Chen, *Eur. J. Med. Chem.* **2018**, *147*, 218. https://doi.org/10.1016/j.ejmech.2018.01.084
[51] C. Cade, P. Swartz, S. H. MacKenzie, A. C. Clark, *Biochemistry* **2014**, *53*(48), 7582. https://doi.org/10.1021/bi500874k
[52] P. Politzer, J. S. Murray, *Theor. Chem. Acc.* **2002**, *108*(3), 134. https://doi.org/10.1007/s00214-002-0363-9
[53] F. J. Luque, M. Orozco, P. K. Bhadane, S. R. Gadre, *J. Phys. Chem.* **2002**, *97*(37), 9380. https://doi.org/10.1021/j100139a021

[54] S. Nayak, S. L. Gaonkar, E. A. Musad, A. M. A. L. Dawsar, *J. Saudi Chem. Soc.* **2021**, *25*(8), 101284. https://doi.org/10.1016/j.jscs.2021.101284
[55] Y. L. Volodina, A. S. Tikhomirov, L. G. Dezhenkova, A. A. Ramonova, A. V. Kononova, D. V. Andreeva, D. N. Kaluzhny, D. Schols, M. M. Moisenovich, A. E. Shchekotikhin, A. A. Shtil, *Eur. J. Med. Chem.* **2021**, *221*, 113521. https://doi.org/10.1016/j.ejmech.2021.113521
[56] M. E. Khalifa, *J. Mol. Struct.* **2020**, *1215*, 128270. https://doi.org/10.1016/j.molstruc.2020.128270
[57] T. Mosmann, *J. Immunol. Methods* **1983**, *65*(1–2), 55. https://doi.org/10.1016/0022-1759(83)90303-4
[58] C. E. Oturanel, I. Kiran, O. Ozsen, G. A. Ciftci, O. Atli, *Anti-Cancer Agent Me* **2017**, *17*(9), 1243. https://doi.org/10.2174/1871520617666170103093923
[59] L. Yurttas, Y. Ozkay, G. Akalin-Ciftci, S. Ulusoylar-Yildirim, *J Enzyme Inhib Med Ch* **2014**, *29*(2), 175. https://doi.org/10.3109/14756366.2013.763253
[60] A. E. Evren, D. Nuha, S. Dawbaa, B. N. Saglik, L. Yurttas, *Eur. J. Med. Chem.* **2022**, *229*, 114097. https://doi.org/10.1016/j.ejmech.2021.114097
[61] A. Daina, O. Michielin, V. Zoete, *Sci. Rep.* **2017**, *7*, 42717. https://doi.org/10.1038/srep42717
[62] C. A. Lipinski, F. Lombardo, B. W. Dominy, P. J. Feeney, *Adv. Drug Deliv. Rev.* **1997**, *23*(1–3), 3. https://doi.org/10.1016/s0169-409x(96)00423-1
[63] Schrödinger Release 2020-3, *Glide*, Schrödinger, LLC, New York, **2020**.
[64] Schrödinger Release 2020-3, *Maestro*, Schrödinger, LLC, New York, **2020**.
[65] Schrödinger Release 2020-1, *LigPrep 2020*, Schrödinger, LLC, New York, **2020**.
[66] A. E. Evren, S. Dawbaa, D. Nuha, Ş.A. Yavuz, Ü.D. GÜL, L. YurttaŞ, *J. Mol. Struct.* **2021**, *1241*, 130692. https://doi.org/10.1016/j.molstruc.2021.130692
[67] M. Frisch, G. Trucks, H. Schlegel, G. Scuseria, M. Robb, J. Cheeseman, G. Scalmani, V. Barone, B. Mennucci, G. Petersson, *Gaussian 09*, *Revision A*, Wallingford CT Inc., **2009**.
[68] R. Dennington, T. Keith, J. Millam, *Gauss View Version* **2009**, *5*. https://gaussian.com/g09citation/
[69] A. Galano, J. R. Alvarez-Idaboy, *J. Comput. Chem.* **2013**, *34*(28), 2430. https://doi.org/10.1002/jcc.23409
[70] A. Galano, J. R. Alvarez-Idaboy, *J. Comput. Chem.* **2014**, *35*(28), 2019. https://doi.org/10.1002/jcc.23715
[71] A. D. Becke, *J. Chem. Phys.* **1992**, *96*(3), 2155. https://doi.org/10.1063/1.462066

SUPPORTING INFORMATION

Additional supporting information can be found online in the Supporting Information section at the end of this article.

How to cite this article: D. Nuha, A. E. Evren, Z. Ş. Çiyanci, H. E. Temel, G. Akalin Çiftçi, L. Yurttaş, *Arch. Pharm.* **2022**;355:e2200105. https://doi.org/10.1002/ardp.202200105